Binding and Uptake of Wheat Germ Agglutinin–Grafted PLGA-Nanospheres by Caco-2 Monolayers

Andrea Weissenboeck,[1] Elisabeth Bogner,[1] Michael Wirth,[1] and Franz Gabor[1,2]

Received February 24, 2004; accepted May 17, 2004

Purpose. The Caco-2 association of lectin-grafted PLGA-nanospheres was investigated compared to plain and BSA-coated spheres.

Methods. Nanospheres made from fluorescent-labeled PLGA were coated with wheat germ agglutinin (WGA) or BSA and incubated with Caco-2 monolayers varying the concentration of nanospheres, the time, and the temperature. The tests were performed in a static horizontal as well as an aerated vertical setup to find out the system most appropriate for estimation of bioadhesion.

Results. Due to bioadhesive effects, WGA-modified particles exhibited highest association to the cells as compared to plain and BSA-coated ones. The amount of associated spheres increased with time and concentration of the nanosphere suspension. Whereas the binding of lectin-coated spheres was independent from energy, their uptake was energy consuming as opposed to BSA and plain nanospheres, which exhibited nonspecific, energy independent binding and uptake. Although more particles were associated with the monolayer in the horizontal setup than in the vertical system, the vertical system reflects true bioadhesion due to circulation of the spheres which inhibits the influence of sedimentation.

Conclusions. Immobilization of WGA considerably enhances the binding as well as the uptake of PLGA-nanospheres by Caco-2 monolayers. For bioadhesion studies, the vertical setup is recommended instead of the horizontal setup.

KEY WORDS: Caco-2; cell-association; lectin; PLGA-nanospheres; wheat germ agglutinin.

INTRODUCTION

Because it is widely accepted that particles are absorbed from the intestine, micro- and nanoparticles are being extensively investigated for peroral delivery of poorly absorbable drugs including peptides, proteins, and DNA (1). Due to its biodegradability and biocompatibility, PLGA is nowadays used not only in medicine as a resorbable suture material and as a scaffold for tissue engineering but also in drug delivery (2–4). By changing the molecular weight and/or the monomer composition of the polymer, the rate of degradation of the particles is altered and allows the controlled release of entrapped drugs (5). In view of the fact that only a small amount of perorally administered spheres is absorbed, sufficient uptake of PLGA particles into cells of the gastrointestine has to be guaranteed prior to practical use (6). On one hand, the size of the particles is crucial for efficient association: *Desai et al.* reported that the uptake of 100-nm particles is 2.5-fold or 6-fold higher than that of 1-μm or 10-μm particles (7). Additionally, microspheres <2 μm were found to be better associated with tissue than microspheres <30 μm and the size limit of uptake was 4 μm (8). On the other hand, because of rather poor bioadhesion of PLGA, binding and uptake into the cells can be facilitated by surface modification of the nanoparticles with lectins (9,10). Lectins are proteins or glycoproteins appropriate for targeting drugs, as they can bind to specific oligosaccharides of the glycocalyx of enterocytes and therefore allow cytoadhesion and cytoinvasion of conjugated drugs (11,12). Especially wheat germ agglutinin (WGA) from *Triticum vulgare* specifically binds to *N*-acetyl-D-glucosamine and sialic acid moieties present at the surface of the human intestine as imitated by Caco-2 monolayers.

The aim of this contribution is to estimate whether both advantageous effects, the cytoadhesive properties of the lectin and the protective effects of the particles, can be combined by conjugation of WGA to the surface of PLGA-nanospheres which might result in improved bioavailability of the formulation (13). As immobilization of WGA at the surface of the spheres requires functional groups, the H-type of the polymer was chosen, which contains free carboxylic groups, as opposed to other types of PLGA carrying alkyl ester end groups (14). To quantify and visualize binding and uptake in Caco-2 monolayers, the nanoparticles were prepared by use of a fluorescent derivative of PLGA. To approach in-vivo conditions, a horizontal and a vertical arrangement of the Caco-2 monolayers was used to estimate the bioadhesivity of the surface engineered nanospheres.

MATERIALS AND METHODS

Materials

Resomer RG 503H (PLGA, lactide/glycolide ratio 50:50, inherent viscosity 0.32–0.44 dl/g, acid number >3 mg KOH/g) was obtained from Boehringer Ingelheim (Ingelheim, Germany). *N*-Hydroxysuccinimide (NHS), bovine serum albumin (BSA), 1-ethyl-3-(3-dimethylaminopropyl)carbodiimide (EDAC), and Pluronic F-68 were purchased from Sigma (Vienna, Austria). *N,N′*-Dicyclohexylcarbodiimide (DCC) and 2-(4-(2-hydroxyethyl)-1-piperazinyl)-ethanesulfonic acid (HEPES) were bought from Merck (Darmstadt, Germany), fluorescein cadaverine (5-((5-aminopentyl)thioureidyl)fluorescein, dihydrobromide salt) was from Molecular Probes (Eugene, OR, USA). Wheat germ agglutinin (WGA) and its fluorescent labeled analog (F-WGA) were obtained from Vector Laboratories (Burlingham, CA, USA) and *N,N′,N″*-triacetylchitotriose from Fluka (Vienna, Austria). All other chemicals used were of analytical purity.

Preparation of Fluorescein-Labeled PLGA

For preparation of fluorescent nanospheres, the fluorescein cadaverine was covalently bound to the polymer. The carboxylic groups of the polymer were activated by mixing 500 μl of each, a 0.4% NHS, 0.51% DCC, and 5.0% PLGA solution in methylene chloride. After end-over–end incubation for 2 h, 500 μl of a solution of 0.73 mg of fluorescein cadaverine in 500 μl dichloromethane and 22 μl pyridine were

[1] Institute of Pharmaceutical Technology and Biopharmaceutics, University of Vienna, Vienna, Austria.

[2] To whom correspondence should be addressed. (e-mail: franz.gabor@univie.ac.at)

added and incubated overnight. The labeled polymer was purified by repeated washings with 5 mM HCl until the aqueous layer remained clear followed by precipitation with methanol for 2 h at 4°C. The fluorescein cadaverine-labeled PLGA (F-PLGA) was lyophilized and stored at 4°C until use.

Preparation of PLGA Nanospheres

The nanospheres were prepared by the double emulsion-technique. Briefly, 200 μl distilled water were emulsified in 1 ml ethylacetate containing 17 mg F-PLGA and 183mg PLGA by sonication for 30 s (sonifier: Bandelin electronic UW 70/HD 70, tip: MS 72/D, Berlin, Germany). After addition of 3 ml 10% (w/v) aqueous Pluronic-solution, the emulsion was sonified again for 25 s. The resulting double-emulsion was poured into 50 ml 1% (w/v) aqueous Pluronic-solution containing 2% isopropanol and maintained under mechanical stirring for 1 h at room temperature. The residual ethylacetate was evaporated under vacuum and the lot was portioned. The aliquots of 1.5 ml each were washed twice with 20 mM HEPES/NaOH pH 7.4 containing 1% Pluronic by centrifugation (Hermle Z323K, 10 min, 8000 rpm, 4°C) and resuspension, and finally stored in 500 μl buffer at –80°C until use.

Surface Modification of the Nanospheres

To activate free accessible carboxylic groups, 500 μl nanosphere-suspension (about 6.5 mg nanospheres) were incubated end-over-end with 500 μl 3.5% EDAC and 500 μl 0.15% NHS in 20 mM HEPES/NaOH pH 7.0 containing 1% Pluronic for 2 h. Excess of crosslinker and by-products were removed by discarding the supernatant after centrifugation. The nanospheres were resuspended in 500 μl buffer and 100 μl 0.1% of WGA or BSA in buffer were added followed by end-over-end incubation for 18 h. To block excess of coupling sites, 100 μl 20% glycine in buffer were added. After incubation end-over-end for 1 h, the particles were washed twice, first with 20 mM HEPES/NaOH pH 7.0 containing 1% Pluronic and secondly with isotonic HEPES/NaOH pH 7.4 containing 1% Pluronic. Finally, the pellet was dispersed in 500 μl isotonic HEPES/NaOH pH 7.4 containing 1% Pluronic and stored at –80°C until use.

Characterization of the Nanospheres

To determine the yield of nanospheres, aliquots of the freshly prepared nanosphere suspension (1.5 ml) were washed twice with distilled water by centrifugation (7000 rpm, 10 min, 4°C) and resuspension followed by freeze drying and weighing.

The F-cadaverine-content was determined fluorimetrically at 485/535 nm after dissolving the nanospheres in 0.1 M NaOH/5% SDS. The calibration curve was established with different concentrations of F-cadaverine in the same solvent.

The mean diameter and the particle size distribution was examined by laser diffraction (Shimadzu Laser Diffraction Particle Size Analyzer SALD-1100, Kyoto, Japan). The nanospheres were suspended in water containing 0.2% Tween 20 as a wetting agent to minimize agglomeration, sonicated for 1min, and analyzed under continuous stirring in duplicate. Sizes were expressed as volume diameters which is indicated by the 90% and the 50% value, meaning that 90% or 50% of the particles are smaller than the given value.

Cell Culture

The Caco-2 cell line was purchased from the American Type Culture Collection (Rockville, MD, USA) and was used between passage 38 and 49. Cells were grown in RPMI-1640 cell culture medium containing 10% fetal calf serum, 4 mM L-glutamine, and 150 μg/ml gentamycine in a humidified 5% CO_2/95% air atmosphere at 37°C, and subcultured by trypsination. For experiments in Ussing chambers, 2 ml cell suspension (129,200 cells/ml) were seeded onto cover glass slides (diameter 19 mm, disinfected with 70% ethanol) in 12-well plates, whereas 1 ml cell suspension containing 136,000 cells/ml was seeded onto cover glass slides (diameter 10 mm, disinfected with 70% ethanol) in 24-well plates for the horizontal setup. Every other day the cell culture medium was exchanged and the tests were performed on confluent monolayers 10 days after seeding.

Experiments in Ussing Chambers

For the experiments in the vertical setup, the glass-slides with adherent monolayers were removed from the 12-well plates, washed with HBSS (Hank's balanced salt solution) and mounted in an Ussing chamber. A calculated amount of plain or surface modified nanospheres in 4.0 ml HBSS (0.5 mg/ml, 1 mg/ml, 1.5 mg/ml, 2 mg/ml, and 2.5 mg/ml) was filled into the donor chamber. The system was aerated with 95% O_2/CO_2 and incubated under protection from light at 4°C or 37°C. After certain time intervals the glass slide was put into a 12-well plate and washed twice with HBSS to remove loosely attached particles. Finally, the monolayer with the associated nanoparticles was dissolved in 500 μl 0.1 N NaOH/5% SDS and the amount of cell-associated particles was determined fluorimetrically at 485/535 nm. Experiments were performed with all types of nanospheres at least in triplicate.

Experiments in the Horizontal Setup

For the experiments in the horizontal setup, the cover glass grown monolayers were removed from the 24-well plates, washed with HBSS and put into a new 24-well plate. After addition of 1.0 ml buffer or nanosphere suspension (0.5 mg/ml, 1 mg/ml, 1.5 mg/ml, 2 mg/ml, or 2.5 mg/ml) in buffer to each well, the plate was incubated at 4°C or 37°C for different time intervals. After washing the glass slide twice with HBSS, the monolayer and the particles were dissolved and the amount of associated particles was determined as described above.

Determination of the Amount of F-cadaverine and Cell Associated Nanospheres

The F-cadaverine content of plain and surface-modified nanoparticles as well as the amount of cell-associated nanospheres was determined by measuring the fluorescence intensity of the nanospheres and/or the monolayer after dissolution in 0.1 N NaOH/5% SDS in a microplate reader (Spectrafluor-reader, Tecan, Grödig, Austria) at 485/535 nm. To guarantee comparability of the results, the amount of cell-associated nanospheres was calculated by means of the F-cadaverine content of the monolayer after dissolution which was correlated to the number of cells/cm^2 monolayer on the glass-slides. The cell number was determined by trypsination of the

monolayer and counting the cells. The assays were performed at least in triplicate.

Carbohydrate-Specificity of Lectinized Nanospheres

To assess the binding specificity of WGA-coated nanospheres, the nanosphere suspension (1mg/ml) was incubated with Caco-2 monolayers in absence and in presence of 500μg and 1000μg *N,N′,N″*-triacetylchitotriose in the vertical and horizontal setup at 4°C for 3 h. The samples were processed as described above.

RESULTS

The stable binding of the fluorescent dye to the polymer molecules as well as the retainment of nanoparticles size distribution during the assay represent two basic requirements for cell-association studies with nanoparticles. As only 6.8 ± 0.2% of the dye were released after incubation in isotonic HEPES/NaOH pH 7.4 containing 1% Pluronic for one week at room temperature, the amide-linkage exhibits sufficient stability to prevent false results. Although the diameter of the nanospheres increased from 0.57 μm to 1.02 μm (90% values) after storage for 6 h at 37°C, the agglomeration of the nanoparticles is supposed to not critically affect their uptake into the monolayer (5,6).

Caco-2 Association of Different Concentrations of WGA, BSA, and Plain Nanospheres

As the assays were performed at 37°C, the term "monolayer-associated nanospheres" refers to bound and internalized nanospheres. Independent from the orientation of the setup, the amount of cell-associated nanospheres increased with the amount of nanospheres added. But the association rate of the spheres was strikingly different being dependent on the type of surface-modification (Fig. 1).

In the vertical setup, the association of plain nanospheres was not detectable at low concentrations and very small at high concentrations which indicates poor cytoadhesive characteristics of PLGA (Fig. 1A). The adhesion and uptake of BSA-grafted spheres was somewhat higher exceeding that of the plain nanospheres 2.7 times at 2 mg/ml. Both types of nonspecific interactions, the polymer-cell and the serum albumin-cell interaction, seemed to reach a plateau ongoing from a concentration of 1.5 mg/ml probably indicating saturation. However, highest association rates were observed in case of WGA-modified nanoparticles. At 2 mg/ml, 25 times more particles as compared to the plain ones or 10 times more nanoparticles as compared to BSA-modified ones were associated with the cells upon coupling the lectin to the surface. Within the concentration range tested no saturation was observed.

When the same assay was performed without convection of the particles by horizontal positioning of the monolayer, overall, the amount of associated nanoparticles was considerably higher (Fig. 1B). At 2 mg/ml a 10-fold (plain particles), 6-fold (BSA-coating), or 2-fold (WGA-coating) higher amount of particles was associated with the monolayer in the horizontal setup than in the vertical setup. However, the difference in association between the diverse coated particles was less distinctive than in the Ussing chamber. After incubation with 2 mg/ml nanoparticles, the amount of associated

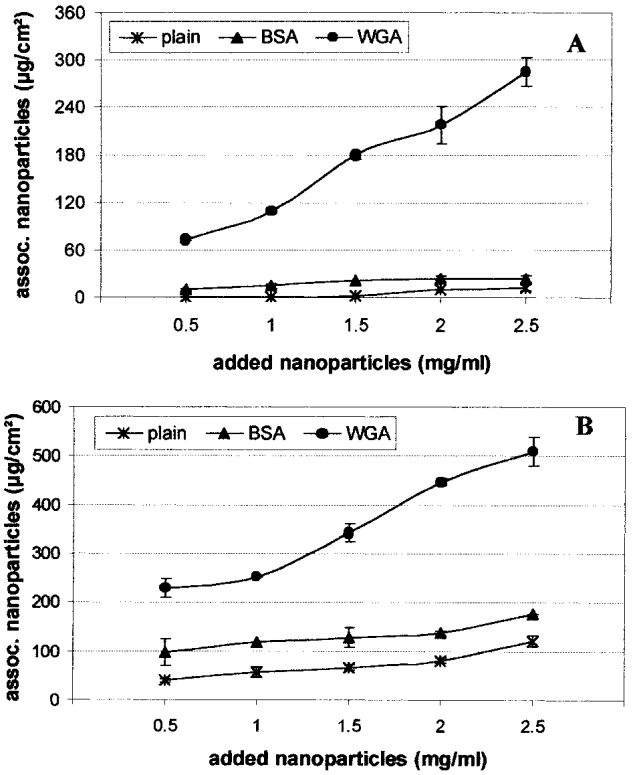

Fig. 1. Association of increasing amounts of plain and surface-modified fluorescent PLGA-nanoparticles with Caco-2 monolayers in the vertical (A) and the horizontal (B) setup.

particles exceeded those of plain particles only 1.7-fold in case of BSA-modification and 5.5-fold upon WGA-modification, respectively. This indicates for strong influence of sedimentation due to lack of movement within the system. Additionally, saturation of binding and uptake was not observed within the concentration range under investigation.

Association of Plain and Modified Particles with Time

When a constant amount of nanoparticles was incubated with the Caco-2 monolayer at 37°C, the amount of nanoparticles associated with the cells increased with time (Fig. 2). But the extent of association was strongly dependent on the positioning of the monolayer, either vertically or horizontally, as well as the surface modification of the nanospheres.

Upon vertical positioning of the monolayer, plain and BSA-grafted particles were associated to a pronounced lesser extent than WGA-grafted spheres (Fig. 2A). Whereas unmodified and BSA-grafted spheres exhibited no Caco-2 binding within the first hour, 40.7 ± 5.6 μg WGA-nanoparticles/cm^2 were associated with the cells, which was about the maximum association rate of the other types of spheres. The nonspecific association of the spheres moderately increased with time, finally resulting in flattening of the curve after 6 h, which might indicate the limit of nonspecific interaction. In contrast, the association of lectin-grafted spheres strongly increased with time even after 6 h suggesting that the cytoadhesive and cytoinvasive characteristics of WGA mediate continuous association of nanoparticles at a high rate.

As observed previously, the total amount of associated spheres was much higher in the horizontal setup than in the

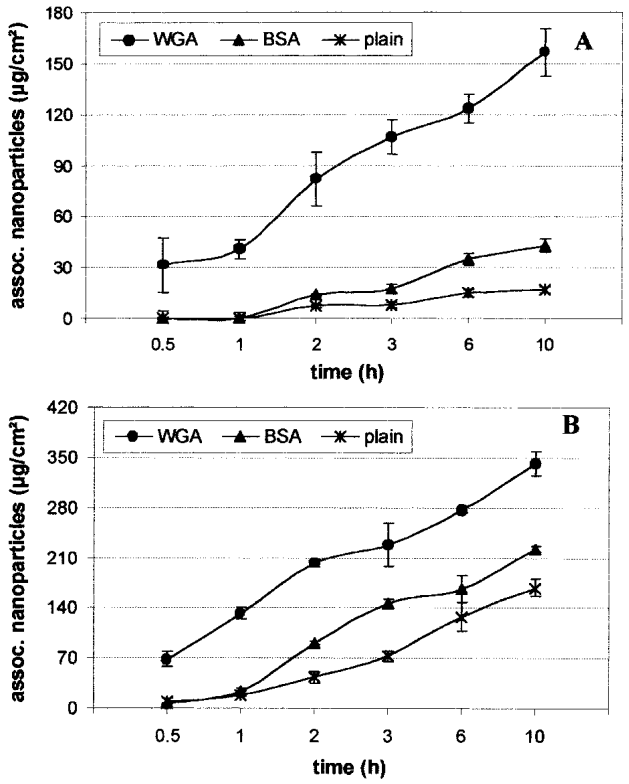

Fig. 2. Association of plain and surface-modified fluorescent PLGA-nanoparticles (1 mg/ml) with Caco-2 monolayers in the vertical (A) and the horizontal (B) setup by course of time.

vertical one (Fig. 2B). Although the association of WGA-grafted spheres was initially considerably higher than that of the others, the WGA/BSA nanoparticle association ratio decreased rapidly with time and reached a steady-state after 3 h, whereas that of the WGA/plain-nanoparticles was observed after 6 h. Probably due to lack of aeration and increased influence of sedimentation the effect of specific bioadhesion on association decreased with prolonged incubation.

Association of Plain and Modified Particles at 4°C and 37°C

Upon incubation at 37°C, the cells are metabolically active and binding as well as energy consuming uptake of nanoparticles can take place. In contrast, at 4°C the fluidity of the cell membrane and the metabolism is reduced so that binding of nanoparticles to the cell membrane is prevailing. Thus, the minimal amount of internalized nanospheres can be calculated from the difference of cell-associated spheres at 37°C and membrane bound spheres at 4°C.

When the spheres were incubated in the vertical setup at 4°C for 3h, WGA-coating mediated the highest binding rate of the nanospheres (Fig. 3A). In comparison, only about a tenth of the nanospheres was bound to the monolayer in case of BSA or plain nanospheres. The same assay, but performed at 37°C, resulted in comparable association rates as observed above. Considering the amount of surface-bound nanospheres, 89.5 ± 0.8 µg/cm² WGA-grafted nanospheres were taken up into the cells at the minimum. In contrast, considerably lower internalization was observed in case of non-specific nanoparticle-cell interactions as represented by uptake of 6.2 ± 0.1 µg/cm² BSA-grafted nanospheres or 2.1 ± 0.1 µg/cm² plain nanospheres. The 3-fold higher uptake of BSA-nanospheres points to qualitative differences of nonspecific interactions. As compared to the negatively charged plain particles made from PLGA with free carboxylic end groups, the interaction of presumably slighter positive charged BSA-nanospheres with the negatively charged cell surface not only resulted in higher binding but also higher uptake.

Upon horizontal positioning of the monolayer, the cell-binding of the various types of nanospheres was not that different as observed in the vertical setup (Fig. 3B). Although WGA-grafted spheres again exhibited highest cell-binding at 4°C, the amount of non-specifically bound nanospheres decreased by only 12.5 ± 18.9% (BSA-nanospheres) or 44.4 ± 9.9% (plain nanospheres). This demonstrates the strong influence of sedimentation on non-specific binding upon horizontal positioning of the monolayer. Calculation of the amount of internalised nanoparticles reveals that at least 100.5 ± 25.1 µg/cm² WGA-coated particles were accumulated within the cells, whereas 31.6 ± 19.8 µg/cm² BSA-coated or 36.5 ± 9.1 µg/cm² plain nanospheres are present in the cell body. Consequently, the binding of the nanoparticles to the cell surface is much stronger influenced by sedimentation than the uptake. The 3-fold higher uptake of lectinised nanospheres reflects the uptake-mediating characteristics of

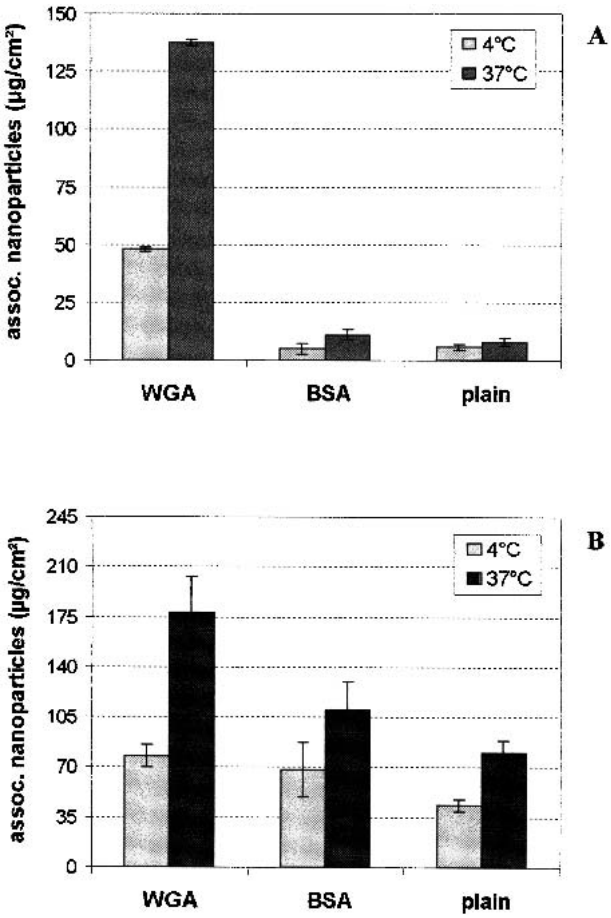

Fig. 3. Binding (4°C) and association (37°C) of plain and surface-modified fluorescent PLGA nanoparticles (1 mg/ml) with Caco-2 monolayers in the vertical (A) and the horizontal (B) setup after incubation for 3 h.

WGA. *Vice versa* the apparently high and rather similar uptake of BSA-coated as well as plain nanospheres points to a similar non-specific mechanism of uptake and facilitated transport into the cells after deposit at the surface which is enhanced by sedimentation.

Carbohydrate Specific Binding of WGA-Coated Nanospheres

In this assay the oligosaccharides of the glycocalyx of the Caco-2 monolayer and the free complementary carbohydrate *N,N′,N″*-triacetylchitriose were allowed to compete for binding to WGA-coated nanopheres (Table I). Independent from the type of setup used, the amount of cell-bound nanospheres decreased with addition of increasing amounts of chitotriose. This points to specific interactions between the cells and the lectinised nanoparticles due to immobilization of carbohydrate-binding pockets at the surface of the nanospheres. But a quantitative difference was observed: In the vertical setup 46.2 ± 3.3% of the nanospheres were inhibited from cell-binding as opposed to only 17.3 ± 4.1% in the horizontal setup after addition of 500 μg chitotriose. The apparently higher inhibitory activity of equal amounts of the complementary carbohydrate in the vertical setup points to preponderance of specific interactions as compared to the horizontal setup. It is likely that the circulation of the nanoparticle suspension in the vertical setup reduces nonspecific interactions and favors specific interactions whereas sedimentation enhances nonspecific binding in the unstirred horizontal setup.

Confocal Laser Scanning Microscopy

To visualize binding and uptake of lectinised nanoparticles by Caco-2 cells, WGA-coated nanoparticles and plain spheres (1 mg/ml) were incubated with single cells at 37°C for 1 h. After removal of unbound particles by repeated washings the cells were analyzed by Confocal Laser Scanning microscopy (Zeiss LSM 410 invert, Zeiss, Jena, Germany).

As depicted by fluorescence images of Caco-2 cells after incubation with plain F-PLGA nanospheres at 37°C, only a few nanospheres were bound and taken up by the cells (Fig. 4). In contrast, when the surface of the fluorescent nanospheres was coated with WGA, the spheres were bound to the cell surface and a huge amount of the spheres is taken up into the cytoplasm. Thus, the cytoadhesive and cytoinvasive characteristics of WGA considerably enhance the uptake of nanospheres into the enterocyte-like Caco-2 cells.

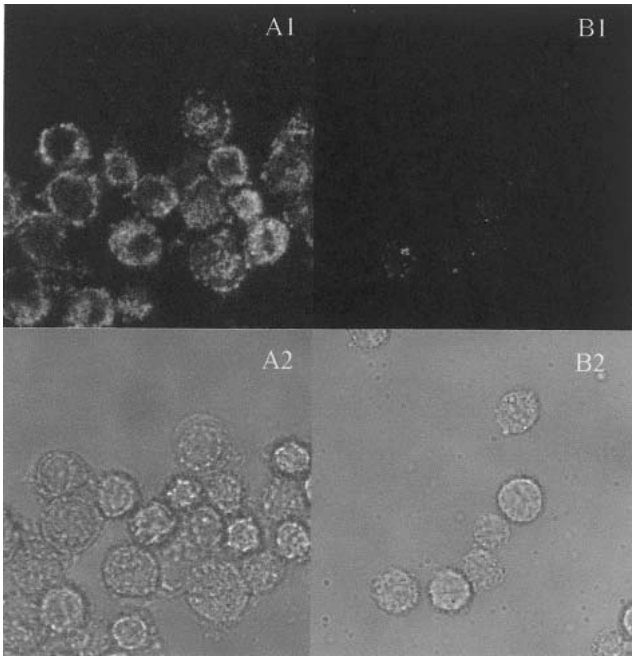

Fig. 4. Confocal images of Caco-2 cells after incubation with WGA-coated (A) and plain (B) fluorescent PLGA nanospheres for 1 h at 37°C. The top row shows the fluorescence (A1, B1), and the bottom row shows the transmission images (A2, B2).

DISCUSSION

Up to now, the uptake of nanoparticles following peroral administration is sufficient for vaccination purposes but it is still to low to reach therapeutical efficacious serum levels of drugs. In an effort to increase the internalisation of colloidal drug carriers, preferentially polystyrene nanoparticles, which are not biodegradable and inappropriate for incorporation of drugs, were surface engineered with vitamin B12, transferrin, folic acid, and tomato lectin (15–18).

In order to take advantage of the biodegradability and the biocompatibility of PLGA as well as the detectability of nanoscaled carriers within the cells, nanoparticles were reported to be loaded with 6-coumarin which released only 0.6% of the dye incorporated (7). In our study, a fluorescent derivative of PLGA was synthesised and used for preparation of fluorescent nanoparticles allowing the adjustment of the fluorescence intensity by mixing labeled and unlabeled polymer according to the sensitivity required for the chosen method. Additionally, leakage of the tag provoked by the first burst effect is repressed due to covalent coupling of the label. Thus, false results can only derive from polymer degradation but not from diffusion of the dye.

According to the literature, the surface of PLGA-nanoparticles can be modified either by activation with polyepoxide/zinc tetrafluoroborate and coupling at acidic pH or

Table I. Competitive Inhibition of the Binding of WGA-Grafted Fluorescent PLGA Nanospheres to Caco-2 Monolayers by Addition of *N,N′,N″*-Triacetylchitotriose

	Vertical system		Horizontal system	
Chitotriose added (μg)	Associated nanoparticles (μg/cm^2)	Inhibition of association (%)	Associated nanoparticles (μg/cm^2)	Inhibition of association (%)
0	41.8 ± 0.1	—	102.1 ± 1.7	—
500	22.5 ± 1.9	46.2 ± 4.5	84.4 ± 0.1	17.3 ± 0.1
1000	15.3 ± 0.9	63.4 ± 2.3	53.9 ± 3.7	47.2 ± 3.7

by surface adsorption of cationic compounds on the anionic nanoparticles (19). In this approach, stable binding of proteinaceous ligands was achieved by activation of free accessible carboxylates at the surface of plain nanoparticles with carbodiimide/*N*-hydroxysuccinimide (20,21). This *N*-hydroxy succinimide ester increases the stability of the active intermediate in aqueous medium and rather rapidly reacts with free amino groups of the ligand than to be subject of hydrolysis. The coupling of either WGA or BSA at neutral pH via amide bonds yielded stable immobilisation of proteinaceous ligands as indicated by loss of only 8.5 ± 0.1% F-WGA after storage in buffer at room temperature for 7 days.

Besides surface charge and hyrophobicity the amount of particles taken up into intestinal epithelia is strongly dependent on size (7,22,23). The nanoparticle size of all the batches used for the association studies ranged between 790 and 1170 nm (90%-value) or between 300 nm and 460 nm (50% value). Any alteration of the size distribution was not observed after surface modification. Additionally, neither plain nor surface engineered nanospheres exerted cytotoxic effects on the viability of the Caco-2 cells as determined by XTT-test after incubation for 2 days at 1.0–7.0 mg/ml (data not shown).

To estimate the bioadhesivity of the nanospheres, two different setups were applied: First, the horizontal setup consisting of horizontal positioned cover-glass grown confluent Caco-2 monolayers with the nanoparticle suspension in the supernatant. This static test arrangement is well described in the literature and is widely used to investigate the interaction of drugs or colloidal formulations with monolayers. Second, a vertical setup consisting of an Ussing chamber with vertical mounted Caco-2 monolayers on cover glass slides was applied. As opposed to the former one, the nanoparticle suspension is circulated by ascending gas bubbles. In this vertical system, containing 5.7×10^6 cells/cm^2, only about 10% of the cells were lost after incubation for 3 h at 37°C. Even more cells, about 14%, were detached from the monolayer in the horizontal setup containing 5.5×10^6 cells/cm^2 prior to the experiment. Consequently, the circulation of the nanosphere suspension exerts no adverse influence on the monolayer and was therefore considered to be negligible.

Within the concentration range tested, the association assays (Fig. 1) in the horizontal setup revealed a considerable but quite different association of all types of nanospheres. However, saturation was not observed. In spite of considerably lower nanoparticle association in the vertical setup, the interaction between plain as well as BSA-grafted nanoparticles and the monolayer was very low and saturable. But binding and uptake of WGA-modified nanospheres increased with concentration. Especially in view of nonexistent adhesion of plain nanoparticles in the vertical system at low concentrations and the remarkable one in the horizontal system it is likely that sedimentation plays a key role in the horizontal system. Thus, the association rate is increased by the test arrangement itself which results in overestimation of the bioadhesivity of plain PLGA-nanoparticles. In the vertical system, however, the nanoparticles are circulated and they only remain attached to the cell membrane when the bioadhesive forces are strong enough to resist the movement of the solvent. The nearly parallel run of the association curves with time in the horizontal system underlines the observation that deposition of nanoparticles at the cell surface facilitates their cell association (Fig. 2). Upon vertical positioning of the cell-layer, the non-specific association reaches a steady state with time, whereas the specific association still increases.

The association studies in the horizontal and the vertical setup underline the bioadhesive characteristics of WGA, even in case of immobilisation on the surface of nanospheres, and the importance of choosing the appropriate test system to estimate bioadhesion. Incubation at different temperatures allowed the assessment of internalized nanospheres, evidently showing that a serious amount of cell-associated WGA-particles is not only bound to the surface but also taken up into the cells by an energy-dependent process. In the vertical setup, the amount of internalised WGA-grafted nanospheres was 14 times higher than that of BSA-grafted or 40 times higher than that of plain nanospheres. This difference decreased to about 3-fold for both BSA and plain nanospheres in the horizontal setup which again reflects the overestimation of non-specific binding and uptake by this technique.

Additionally, the involvement of the carbohydrate binding motif present at the surface of the WGA-grafted spheres was confirmed by a competitive assay with chitotriose. Upon addition of the inhibitory carbohydrate up to 63.4% less spheres were bound in the vertical system, whereas in the horizontal system it was up to 47.2%. Consequently, application of the horizontal setup leads to underestimation of specific bioadhesive interactions.

Among the *ex vivo* models for measuring the bioadhesion of particles to viable tissue such as the microtensitometer or the electromagnetic force transducer, which requires magnetic microparticles, a simple vertical setup of Caco-2 monolayers and fluorescent particles is proposed as an additional tool to estimate the benefits of surface engineered nanoparticles. (24,25). Whereas the static horizontal device suffers from deposition of particles and overestimation of bioadhesion, the rather "true bioadhesion" is determined using a vertical mounted artificial tissue and circulating nanoparticles. Additionally, competitive assays and different incubation temperatures not only allow discrimination between specific and non-specific binding but also between binding and uptake of the submicron particles.

In vascular smooth muscle cells, plain PLGA-nanospheres were reported to be taken up in part through fluid phase pinocytosis and in part through clathrin-coated pits (4). According to the assays in the vertical setup as well as the CLSM of single cells, in epithelial Caco-2 cells the internalisation of plain PLGA-nanospheres is nonspecific and rather low. But surface modification with WGA considerably increased the cytoadhesion and cytoinvasion of the PLGA-nanoparticles. As WGA binds to the EGF-receptor and enhanced cellular uptake of conjugated proteins was predominantly due to the EGF-WGA interaction, the energy dependent uptake of WGA-grafted nanospheres points to opening of a receptor-mediated pathway even for nanoparticles (26,27). According to the CLSM-images of cell-associated lectinised nanospheres the huge amount of internalised particles might be sufficient to provoke therapeutically relevant plasma levels of drugs incorporated. Furthermore, about 60% of water-soluble protein-WGA conjugates were found to be accumulated and degraded in the lysosomal compartment (28). As opposed to WGA-prodrugs the shuttled drugs are expected to be protected within the matrix preventing premature inactivation prior to their pharmacological effect. Additionally, PLGA-nanospheres escape the endo-lysosmes and

enter the cytosolic compartment within 10 min after incubation, which is due to reversal of the negative surface charge selectively at the acidic pH of endo-lysosomes (4,29). Provided that the zeta potential of the lectinised nanospheres is not altered considerably by surface immobilisation of WGA, the WGA-grafted nanospheres are expected to shuttle a huge amount of drugs incorporated undamaged to the cytoplasm.

All in all, the surface engineering of nanoparticles with WGA opens a receptor-mediated pathway for uptake of nanoparticles which improves the cytoadhesion as well cytoinvasion of biodegradable PLGA-nanoparticles. Due to the specific and strong biorecognitive interaction between lectinised nanoparticles and the cell surface, the binding to the cell surface is expected to rather resist the high motility in the intestine and to be less influenced by foodstuff. The EGF-receptor mediated endocytosis provided by the lectin-coat facilitates overcoming the epithelial barrier so that WGA-grafted nanoparticles might be useful delivery systems for conventional poorly bioavailable as well as new biotech drugs to achieve efficacious plasma levels.

ACKNOWLEDGMENTS

A. Weissenboeck was supported by a research fellowship from the University of Vienna

REFERENCES

1. A. T. Florence. The oral absotprion of micro- and nanoparticulates: Neither exceptional nor unusual. *Pharm. Res.* **14**:259–266 (1997).
2. A. A. Ignatius and L. E. Claes. *In vitro* biocompatibility of bioresorbable polymers: poly(L,DL-lactide) and poly(L-lactide-co-glycolide). *Biomaterials* **17**:831–839 (1996).
3. H. R. Lin, C. J. Kuo, C. Y. Yang, S. Y. Shaw, and Y. J. Wu. Preparation of macroporous biodegradable PLGA scaffolds for cell attachment with the use of mixed salts as porogen additives. *J. Biomed. Mater. Res.* **63**:271–279 (2002).
4. J. Panyam and V. Labhasetwar. Biodegradable nanoparticles for drug and gene delivery to cells and tissue. *Adv. Drug Del. Rev.* **55**:329–347 (2003).
5. J. M. Anderson and M. S. Shive. Biodegradation and biocompatibility of PLA and PLGA microspheres. *Adv. Drug Del.Rev.* **28**: 5–24 (1997).
6. G. J. Russell-Jones, H. Veitch, and L. Arthur. Lectin-mediated transport of nanoparticles across Caco-2 and OK cells. *Int. J. Pharm.* **190**:165–174 (1999).
7. M. P. Desai, V. Labhasetwar, E. Walter, R. J. Levy, and G. L. Amidon. The mechanism of uptake of biodegradable microparticles in Caco-2 cells is size dependent. *Pharm. Res.* **14**:1568–1573 (1997).
8. S. McClean, E. Prosser, and E. Meehan. D. ÓMalley, N. Clarke, Z. Ramtoola, and D. Brayden. Binding and uptake of biodegradable poly-DL-lactide micro-and nanoparticles in intestinal epithelia. *Eur. J. Pharm. Sci.* **6**:153–163 (1998).
9. N. Hussain, P. U. Jani, and A. T. Florence. Enhanced oral uptake of tomato lectin-conjugated nanoparticles in the rat. *Pharm. Res.* **14**:613–618 (1997).
10. E. Mathiowitz, J. S. Jacob, Y. S. Jong, G. P. Carino, D. E. Chickering, P. Chaturvedi, C. A. Santos, K. Vijayaraghavan, S. Montgomery, M. Bassett, and C. Morrell. Biologically erodable microspheres as potential oral drug delivery systems. *Nature* **386**:410–414 (1997).
11. F. Gabor, M. Wirth, B. Jurkovich, I. Haberl, G. Theyer, G. Walcher, and G. Hamilton. Lectin-mediated bioadhesion: Proteolytic stability and binding-characteristics of *wheat germ* agglutinin and *Solanum tuberosum* lectin on Caco-2, HT-29 and human colonocytes. *J. Control. Rel.* **49**:27–37 (1997).
12. M. Wirth, C. Kneuer, C. M. Lehr, and F. Gabor. Lectin-mediated drug delivery: discrimination between cytoadhesion and cytoinvasion and evidence for lysosomal accumulation of wheat germ agglutinin in the Caco-3 model. *J. Drug Targ.* **10**:439–448 (2002).
13. B. Ertl, F. Heigl, M. Wirth, and F. Gabor. Lectin-mediated bioadhesion: preparation, stability and Caco-2 binding of wheat germ agglutinin-functionalized poly(D,L-lactic-co-glycolic acid)-microspheres. *J. Drug Targ.* **8**:173–184 (2000).
14. B. Ertl, P. Platzer, M. Wirth, and F. Gabor. Poly(D,L-lactic-co-glycolic acid) microspheres for sustained delivery and stabilization of camptothecin. *J. Control. Rel.* **61**:305–317 (1999).
15. G. J. Russell-Jones, L. Arthur, and H. Walker. Vitamin B_{12}-mediated transport of nanoparticles across Caco-2 cells. *Int. J. Pharm.* **179**:247–255 (1999).
16. Y. Li, M. Ogris, E. Wagner, J. Pelisek, and M. Rueffer. Nanoparticles bearing polyethylenglycol-coupled transferrin as gene carriers: preparation and in vitro evaluation. *Int. J. Pharm.* **259**: 93–101 (2003).
17. Y. Zhang, N. Kohler, and M. Zhang. Surface modification of superparamagnetic magnetite nanoparticles and their intracellular uptake. *Biomaterials* **23**:1553–1561 (2002).
18. N. Hussain, P. U. Jani, and A. T. Florence. Enhanced oral uptake of tomato lectin-conjugated nanoparticles in the rat. *Pharm. Res.* **14**:613–618 (1997).
19. V. Labhetswar, C. Song, W. Humphrey, R. Shebuski, and R. J. Levy. Arterial uptake of biodegradable nanoparticles: Effect of surface modifications. *J. Pharm. Sci.* **87**:1229–1234 (1998).
20. J. V. Staros, R. W. Wright, and D. M. Swingle. Enhancement by N-hydroxysulfosuccinimide of water-soluble carbodiimide-mediated coupling reactions. *Anal. Biochem.* **156**:220–222 (1986).
21. D. G. Hoare and D. E. Koshland Jr. A Method for the Quantitative Modification and Estimation of Carboxylic Acid Groups in Proteins. *J. Biol. Chem.* **242**:2447–2453 (1967).
22. T. Jung, W. Kamm, A. Breitenbach, E. Kaiserling, J. X. Xiao, and T. Kissel. Biodegradable nanoparticles for oral delivery of peptides: is there a role for polymers to affect mucosal uptake? *Eur. J. Pharm. Biopharm.* **50**:147–160 (2000).
23. M. P. Desai, V. Labhasetwar, G. Amidon, and R. J. Levy. Gastrointestinal uptake of biodegradable microparticles: effect of particle size. *Pharm. Res.* **13**:1838–1845 (1996).
24. D. E. Chickering III, C. A. Santos, and E. Mathiowitz. Adaption of a microbalance to measure bioadhesive properties of microspheres. In E. Mathiowitz, D.E. Chickering III, and C.M. Lehr (eds.), *Bioadhesive Drug Delivery Systems*, Marcel Dekker, New York, 1999, pp. 131–146.
25. B. A. Hertzog and E. Mathiowitz. Novel magnetic technique to measure bioadhesion. In E. Mathiowitz, D.E. Chickering III, and C.M. Lehr (eds.), *Bioadhesive Drug Delivery Systems*, Marcel Dekker, New York, 1999, pp. 147–173.
26. N. Lochner, F. Pittner, M. Wirth, and F. Gabor. Wheat germ agglutinin binds to the epidermal growth factor of artificial Caco-2 membranes as detected by silver nanoparticle enhanced fluorescence. *Pharm. Res.* **20**:833–839 (2003).
27. F. Gabor, E. Bogner, A. Weissenboeck, and M. Wirth. The lectin-cell interaction and its implications to intestinal lectin-mediated drug delivery. *Adv. Drug Del. Rev.* **56**:459–480 (2004).
28. F. Gabor, A. Schwarzbauer, and M. Wirth. Lectin-mediated drug delivery: Binding and uptake of BSA-WGA conjugates using the Caco-2 model. *Int. J. Pharm.* **237**:227–239 (2002).
29. J. Panyam, W. Zhou, S. Prabha, S. K. Sahoo, and V. Labhasetwar. Rapid endo-lysosomal escape of poly(D,L-lactide-co-glycolide) nanoparticles: implications for drug and gene delivery. *FASEB J.* **16**:1217–1226 (2002).